Higher-order finite-difference pseudopotential method: An application to diatomic molecules

James R. Chelikowsky
Department of Chemical Engineering and Materials Science and the Minnesota Supercomputer Institute, University of Minnesota, Minneapolis, Minnesota 55455

N. Troullier
Department of Chemical Engineering and Materials Science, Department of Computer Science, and the Minnesota Supercomputer Institute, University of Minnesota, Minneapolis, Minnesota 55455

K. Wu and Y. Saad
Department of Computer Science and the Minnesota Supercomputer Institute, University of Minnesota, Minneapolis, Minnesota 55455
(Received 2 June 1994)

We present a prescription for performing electronic-structure calculations without the explicit use of a basis. Our prescription combines a higher-order finite-difference method with *ab initio* pseudopotentials. In contrast to methods that combine a plane-wave basis with pseudopotentials, our calculations are performed completely in real space. No artifacts such as supercell geometries need be introduced for localized systems. Although this approach is easier to implement than one that employs a plane-wave basis, no loss of accuracy occurs. We apply this method to calculate the structural and electronic properties of several diatomic molecules: Si_2, C_2, O_2, and CO.

I. INTRODUCTION

One of the most successful methods for calculating the structural and electronic properties of condensed-matter systems is based on combining pseudopotentials with a plane-wave basis.[1] Only the valence electrons are considered with this method. The resulting pseudopotential is weaker (usually nonsingular) as compared to the all-electron potential, and converges rapidly in Fourier space. Since the resulting pseudo-wave-function solutions for the isolated atom are smooth, and often nodeless, plane waves are often a reasonable basis. For crystalline materials such as silicon, or gallium arsenide, less than a hundred plane waves per atom are needed for a converged solution.[1] However, for localized systems such as clusters,[2,3] disordered systems such as liquids or glasses,[4,5] or semiperiodic systems such as surfaces[6,7] the direct application of a plane-wave basis is nontrivial. The lack of periodicity in these materials invalidates Bloch's theorem, and the implementation of Fourier transforms. One procedure to "rescue" the plane-wave basis is the *supercell method*.[1] In the supercell method, the localized configuration of interest is artificially repeated to impose periodicity on the system. For example, if one wanted to examine a molecule, the molecule would be isolated in a large cell, and this cell would be artificially repeated to construct a crystal of isolated molecules. This forced periodicity of supercells allows standard band structure codes to be used for nonperiodic systems.

The drawbacks of the plane-wave–supercell approach are notable. The plane-wave basis is required to replicate not only the electronic states of the localized system of interest, but also vacuum regions imposed by the supercell geometry. Replicating the vacuum in the supercell for a localized system can be almost as costly as replicating the "real" part of the wave function. In a recent calculation for a complex surface, the 7×7 reconstruction of the (111) silicon surface, 700 atoms were effectively treated: approximately 400 "real" atoms in the supercell and a vacuum contribution effectively corresponding to another 300 atoms.[6,7]

Another issue which complicates supercell calculations concerns interactions from one cell into another. For example, one can examine a vacancy in a crystal by considering a large supercell of the ideal crystalline solid and removing an atom from the supercell. If one wishes to examine charged systems, the problem becomes more acute. Consider a charged defect within a supercell configuration; for this situation each individual cell is charged. The total electronic energy summed over all the cells diverges. A simple "fix" to this problem is to insert a uniform compensating charge in each supercell, but determining the effect of this uniform background in terms of a total energy, or binding energy, is highly nontrivial.[8,9]

An additional complication that arises with the use of plane waves concerns the use of fast Fourier transforms (FFT) for handling the convolutions. While FFT's are a great advantage in expediting the calculation, these transforms present computational communication obstacles when one attempts to implement FFT-based codes on parallel computer architectures.

Here we present an approach which eliminates these problems. Our approach is much simpler to implement than the plane-wave basis without any loss of accuracy. The approach is based on utilizing the *higher-order finite-difference method*.[10,11] In the finite-difference method the unknown variables are the wave functions on

0163-1829/94/50(16)/11355(10)/$06.00

a discrete grid. Within this approach, the "discrete" real space grid is the *basis*. Derivatives are approximated by a function which sums over the weighted value of the wave function at the neighboring points. It might be suspected that a grid approach would not be competitive with other approaches such as plane waves. The real-space grid must be fine enough to replicate accurately the wave functions. A grid this fine may result in so many points as to result in an unworkable scheme. If one considers an all-electron potential it has a singularity at the origin. A simple regularly spaced grid which is fine enough near the singularity to describe the core states would be "too fine" and wasteful for the outer "chemistry" regions of the valence states. This situation need not be the case, especially when the finite-difference method is coupled with pseudopotentials. The pseudopotential is finite at the origin, and the resulting wave functions are *smoothly varying functions*. A simple, uniform grid may be sufficient in this situation.

The two approaches, i.e., plane-wave expansions and finite-difference descriptions, are intimately related. If the wave function is slowly varying, then it should be easy to expand the function in a plane-wave basis. Likewise, for a slowly varying function, the wave function can be expanded locally in a Taylor series, and a finite-difference method using relatively few discretization points will work well. This will be especially true for a higher-order finite-difference method.

The use of standard (low order) finite differences to solve the Schrödinger equation and other related wave equations has a long history. In the mid-1930s, Kimball and Shortley used it to solve for the wave functions of the hydrogen atom.[12] The method was applied[13] sparingly in the late 1930s and 1940s and has appeared sporadically since then. Solving the entire problem in real space is not a novel feature, and in this respect our method closely resembles the discrete variational method of Ellis and coworkers[14] and the discrete variable representation approach of Lill, Parker, and Light.[15] Here we combine a higher-order finite difference with the pseudopotential method on a real space without the explicit use of a basis set. The smoothness of the pseudopotential and pseudowave functions, the accuracy of the higher-order finite-difference expansion, and the simplicity of a real-space discrete grid creates a method which is easy to use, flexible, efficient, and as accurate as the plane-wave method.

To illustrate the higher-order finite-difference pseudopotential method, we examine the electronic-structure problem for simple diatomic molecules. The electronic structure of small molecules presents a severe challenge to plane-wave approaches. The plane-wave approach is not only required to describe localized systems where the wave functions are compact, but also the vacuum regions where the wave functions vanish. In order to accurately accomplish this with plane waves, the supercell used must be quite large so as not to allow the wave functions and the screening potentials from neighboring cells to overlap. We have chosen to examine Si_2, C_2, O_2, and CO. Determining the electronic structure of the O_2 molecule is challenging owing to a large nonlocal component, and the localized nature of the valence states. The CO molecule is also challenging. The dipole moment of this molecule changes sign with small changes in the bond length. We have calculated the structural and electronic properties of these molecules with a finite-difference approach and with a plane-wave basis. We also compare these results to a number of previous calculations.

II. COMPUTATIONAL METHODS

A key aspect of our work is the availability of higher-order expansions for the kinetic-energy operator, i.e., expansions of the Laplacian. We impose a simple, uniform orthogonal three-dimensional (3D) grid on our system where the points are described in a finite domain by (x_i,y_j,z_k).[16] We approximate $\partial^2\psi/\partial x^2$ at (x_i,y_j,z_k) by

$$\frac{\partial^2\psi}{\partial x^2}=\sum_{n=-N}^{N} C_n\psi(x_i+nh,y_j,z_k)+O(h^{2N+2}) , \qquad (1)$$

where h is the grid spacing and N is a positive integer. This approximation is accurate to $O(h^{2N+2})$ upon the assumption that ψ can be approximated accurately by a power series in h. Algorithms are available to compute the coefficients C_n for arbitrary order in h.[17] Expansion coefficients for a uniform grid are given in Table I for $N\leq 6$.

With the kinetic-energy operator expanded as in Eq. (1), one can set up a one-electron Schrödinger equation over the grid. We will employ the local-density approximation in setting up the Schrödinger equation. We solve for $\psi(x_i,y_j,z_k)$ on the grid by solving the secular equation:

TABLE I. Expansion coefficients C_n, $n=0,\ldots,\pm N$, for higher-order finite-difference expressions of the second derivative.

	C_i	$C_{i\pm1}$	$C_{i\pm2}$	$C_{i\pm3}$	$C_{i\pm4}$	$C_{i\pm5}$	$C_{i\pm6}$
$N=1$	-2	1					
$N=2$	$-\frac{5}{2}$	$\frac{4}{3}$	$-\frac{1}{12}$				
$N=3$	$-\frac{49}{18}$	$\frac{3}{2}$	$-\frac{3}{20}$	$\frac{1}{90}$			
$N=4$	$-\frac{205}{72}$	$\frac{8}{5}$	$-\frac{1}{5}$	$\frac{8}{315}$	$-\frac{1}{560}$		
$N=5$	$-\frac{5269}{1800}$	$\frac{5}{3}$	$-\frac{5}{21}$	$\frac{5}{126}$	$-\frac{5}{1008}$	$\frac{1}{3150}$	
$N=6$	$-\frac{5369}{1800}$	$\frac{12}{7}$	$-\frac{15}{56}$	$\frac{10}{189}$	$-\frac{1}{112}$	$\frac{2}{1925}$	$-\frac{1}{16\,632}$

$$-\frac{\hbar^2}{2m}\left[\sum_{n_1=-N}^{N} C_{n_1}\psi(x_i+n_1h,y_j,z_k)+\sum_{n_2=-N}^{N} C_{n_2}\psi(x_i,y_j+n_2h,z_k)+\sum_{n_3=-N}^{N} C_{n_3}\psi(x_i,y_j,z_k+n_3h)\right]$$
$$+[V_{\rm ion}(x_i,y_j,z_k)+V_H(x_i,y_j,z_k)+V_{\rm xc}(x_i,y_j,z_k)]\psi(x_i,y_j,z_k)=E\psi(x_i,y_j,z_k)\ . \quad (2)$$

If there are M grid points, the size of the full matrix resulting from the above eigenvalue problem is $M\times M$. $V_{\rm ion}$ is the nonlocal ionic pseudopotential, V_H is the Hartree potential, and $V_{\rm xc}$ is the local-density expression for the exchange and correlation potential. The two parameters used in setting up the matrix are the grid spacing h, and the order N.

Several issues must be addressed to solve Eq. (2). The first concerns the procedure by which the self-consistent field, i.e., the Hartree and exchange-correlation potentials, is constructed. The exchange-correlation potential $V_{\rm xc}$ is a functional of the local charge density. Once the density is determined on a grid point, $V_{\rm xc}$ depends only on the charge density at that point. We use the Ceperley-Alder form as parametrized by Perdew and Zunger[18] for $V_{\rm xc}$. Another issue concerns the construction of the Hartree potential. For small simple isolated systems, we can solve for V_H by direct numerical summation over the grid. We evaluate V_H on the ijk grid points by assuming the integrand does not change appreciably within a cube of volume h^3 around each grid point. V_H is given by

$$V_H(x_i,y_j,z_k)=\sum_{i'j'k'}\rho(x_i',y_j',z_k')\times g(x_i-x_{i'},y_j-y_{j'},z_k-z_{k'})\ , \quad (3)$$

where for $ijk\neq i'j'k'$

$$g(x_i-x_{i'},y_j-y_{j'},z_k-z_{k'})=\frac{h^3}{\sqrt{(x_i-x_{i'})^2+(y_i-y_{i'})^2+(z_i-z_{i'})^2}}\ ,$$

and for $ijk=i'j'k'$

$$g(0,0,0)=-h^2\left[\frac{\pi}{2}+3\ln\left[\frac{\sqrt{3}-1}{\sqrt{3}+1}\right]\right]\ .$$

Near the square root singularity, which occurs at $ijk=i'j'k'$, we have performed an explicit integration over the cube. We find this simple procedure is efficient, yet accurate, for small clusters. As the clusters become larger, e.g., ten atoms or more, it eventually becomes more efficient to solve the Poisson equation using a matrix formalism coupled to the higher-order finite-difference method. To set up the matrix, one needs to determine the boundary conditions; i.e., the values of the potential just outside of the domain. We obtain these by the use of a multipole expansion for the charge density, or using the direct summation scheme outlined above. This matrix equation can be solved by iterative subspace methods, in a similar manner used to determine the eigenvalues and eigenfunctions of the Hamiltonian matrix.[19] This is a straightforward procedure which requires essentially no increase in memory and is easily extended to periodic systems.[20] We used a Broyden mixing scheme to expedite the convergence of the self-consistent field.[19,21]

Nonlocality in the ionic pseudopotential corresponds to an angular momentum-dependent projection term. We construct these ionic pseudopotentials as we would for any electronic structure calculation. Details of their construction can be found elsewhere.[22] The core radii which define the pseudopotentials here are given in Table II. We employ the Kleinman-Bylander[23] form in *real space*[24] for the nonlocal ionic potentials:

$$V_{\rm ion}(x,y,z)\psi(x,y,z)=V_{\rm loc}(x,y,z)\psi(x,y,z)+\sum_{lm}G_{lm}u_{lm}(x,y,z)\Delta V_l(x,y,z)\ , \quad (4)$$

where

$$G_{lm}=\frac{\int u_{lm}(x,y,z)\Delta V_l(x,y,z)\psi(x,y,z)dx\,dy\,dz}{\int u_{lm}(x,y,z)\Delta V_l(x,y,z)u_{lm}(x,y,z)dx\,dy\,dz}\ , \quad (5)$$

where ψ is the wave function, $V_{\rm loc}$ is the local ionic pseudopotential, $\Delta V_l=V_l-V_{\rm loc}$ is the difference between other l components of the ionic and the local ionic potential. The functions u_{lm} are solutions to the atomic pseudopotential for the valence states of interest. Usually, one component is taken as the local component. Here we take $V_l=V_s$, where V_s is the s component. For the systems of interest, we may ignore contributions to the potential higher than $l=1$. The range of ΔV_l is usually much less than a bond length. The nonlocality in $V_{\rm ion}$ is reflected by the occurrence of $\psi(x,y,z)$ in G_{lm}. The integral involving $\psi(x,y,z)$ is performed by a direct summation over the relevant grid points, i.e.,

TABLE II. Core radii (in a.u.) for the ionic pseudopotential construction.

Atom	r_s	r_p
Silicon	2.50	2.50
Oxygen	1.30	1.65
Carbon	1.45	1.45

$$\int u_{lm}(x,y,z)\Delta V_l(x,y,z)\psi(x,y,z)dx\,dy\,dz$$

$$=\sum_{ijk} u_{lm}(x_i,y_j,z_k)\Delta V_l(x_i,y_j,z_k)\psi(x_i,y_j,z_k)h^3 \ . \tag{6}$$

The local potential resides only on the diagonal; only the diagonal part of the matrix needs to be updated during the self-consistency iterations. The full matrix for these isolated systems is real, symmetric, and sparse. These attributes can be utilized in expediting the diagonalization procedure. The sparsity of the matrix is a function of the order N to which the kinetic energy is expanded. We have employed an iterative subspace diagonalization[19] procedure which can take advantage of the sparsity to solve for the eigenvalues and vectors. An alternate approach to using the sparsity in performing the matrix vector products is to leave the matrix in operator format. Using this procedure, there is no need to store the matrix in any sparse form since the coefficients C_{n_i}, $i=1,2,3$; $n=-N,N$ in Eq. (2) are constant and as a result, the matrix-by-vector kinetic operations required by the diagonalization routine can be performed in "stencil" form. The nonlocal operations are accomplished by performing them as vector-by-vector operations. This strategy not only saves storage, it leads to an efficient implementation on most high-performance vector and parallel computers.

In performing calculations for the structural and electronic properties of these molecular systems, three items need to be determined: the domain to contain the atoms or molecule, the order N for the kinetic-energy expansion, and the grid spacing, h. We start our calculations by solving for the electronic structure of the isolated atoms by direct integration. Given the pseudoatom wave functions, we choose a radius, $R_{\max}$ beyond which we expect the atomic states to vanish. Typically this radius encompasses at least 99% of the valence charge. We chose $R_{\max}$ to be 6.8 a.u. for Si and 5.6 a.u. for C and O (1 a.u.=0.529 Å). The domain for a molecular system is then constructed by requiring all atoms of interest to reside at least $R_{\max}$ from a surface.

In the *standard* finite-difference method, the order N is fixed (at $N=1$) and the mesh size h is varied to obtain a desired accuracy. Typically to determine the accuracy, the results of two meshes are compared (h and $h/2$), and an estimate of the error is then determined. A more appropriate mesh-spacing h can then be derived, if necessary. Since we have knowledge of the eigenvalues and the pseudo-wave-functions as determined by a direct integration of the atomic pseudopotentials, we can use this information to compare with the results obtained by the finite-difference method. We have two parameters, N and h, to obtain the desired accuracy. To find these we start with a large grid spacing and continuously reduce h until the eigenvalues and wave functions are replicated. We have verified this procedure for several orders of N, in Eq. (1).

Let us illustrate this procedure for the oxygen atom. Given the localized nature of the oxygen wave functions, this atom should be a severe test. In Fig. 1, we illustrate the convergence of the eigenvalues as a function of h for several values of N. For the "standard" finite-difference method, $N=1$, the eigenvalues have not converged to the known values even for $h=0.35$ a.u. At this value of h, the eigenvalues differ by more than 0.1 Ry from those determined by direct integration. However, for $N\geq 4$, the eigenvalues are converged to within 0.01 Ry for $h\leq 0.4$. We have experimented with higher values of N, i.e., with $N=6$–9. We find that for most applications, orders higher than $N=6$ do not provide significant improvement. For example, if N is increased from 6 to 9, the total electronic energy of the oxygen atom changes by less than ~ 0.005 Ry for $h=0.4$ a.u. All of the following calculations reported have been done with $N=6$. The grid spacing was taken to be $h=0.75$ a.u. for silicon, and $h=0.4$ for carbon and oxygen.

As a test of the Hartree potential, we illustrate this potential in Fig. 2 for the oxygen atom as calculated by a direct integration and by a summation procedure as in Eq. (3). The only significant difference resides at the origin: away from the origin the largest difference is less than ~ 0.01 Ry. The difference at the origin is ~ 0.2 Ry. While this is a relatively large difference, it is not an important correction as it is confined to a small region of space.

The Hamiltonian matrix size obtained by the finite-

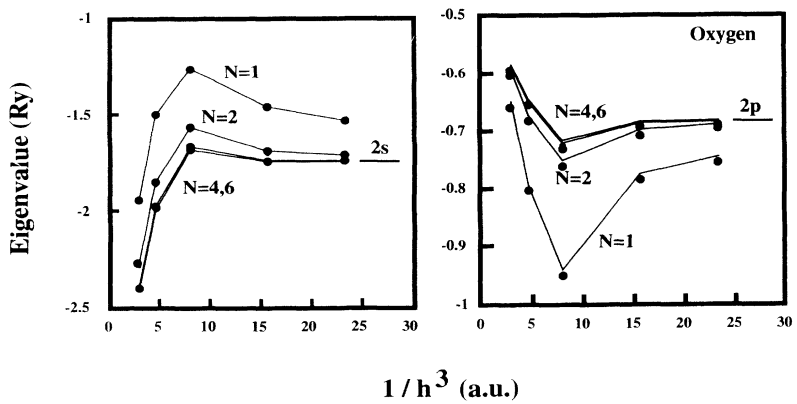

FIG. 1. Behavior of the 2s and 2p eigenvalues for oxygen as a function of the grid spacing parameter h and the finite-difference expansion parameter N. The size of the resulting matrix correlates with $1/h^3$.

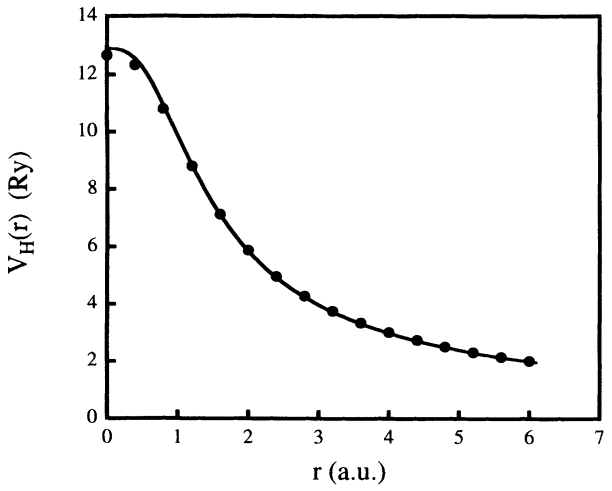

FIG. 2. The atomic oxygen Hartree potential from a self-consistent field calculation using a direct integration method, solid line, and using higher-order finite difference and the summation procedure as in Eq. (3), filled dots.

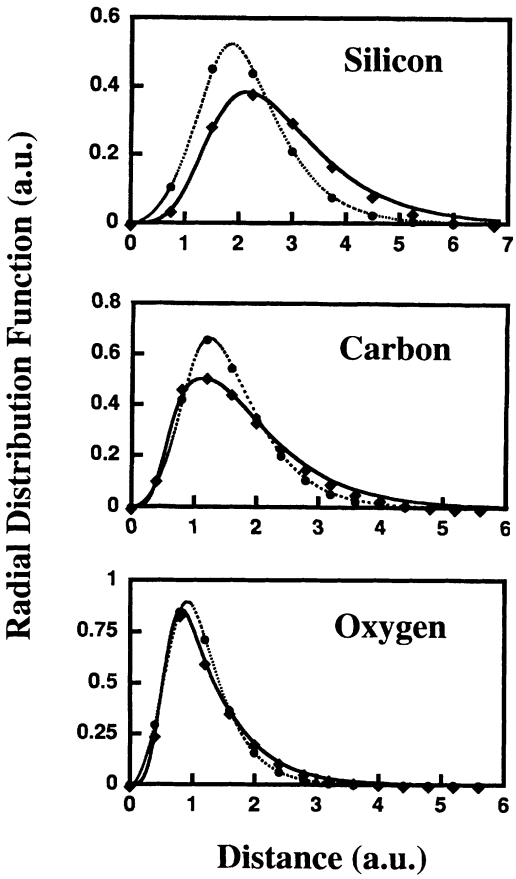

FIG. 3. Radial pseudo-wave-function distributions for silicon, carbon, and oxygen for the s state (dashed line) and p state (solid line). The solid points correspond to a finite-difference description for the s state (●) and the p state (♦).

difference pseudopotential method is comparable with that obtained using plane waves. The full Hamiltonian matrix size for the silicon dimer is approximately 4000×4000. The matrix size for the carbon, and oxygen diatomics, and the CO molecule is approximately $14\,000\times14\,000$. We need not store the full matrix as mentioned previously. The nonzero elements of the Hamiltonian matrix were on the average 13–14 per row and/or column for all the molecules studied.

In Table III, we list the pseudopotential eigenvalues from the direct integration of the atomic Schrödinger equation for Si, C, and O, and as calculated using the finite-difference method. The largest error in the eigenvalues is on the order of ~0.02 Ry. This is the type of error which one would introduce by using a plane-wave basis and the supercell method. As a test of the atomic wave functions from our finite-difference method, we have calculated the lowest excitations for the atomic species of interest: a $^3P\rightarrow{}^1D$ transition. Using local-density spin-polarization formalism, we compare to measured atomic spectra.[26] In Fig. 3, we illustrate the wave function from finite-difference calculations, and compare the wave functions from direct integration. It is perhaps somewhat surprising that these wave functions are so accurate given that only ~10–15 points are considered along a given axis.

TABLE III. Atomic energy levels (in Ry) from pseudopotentials by direct integration (DI) and from finite-difference calculations (FD). Also, the lowest excitation (in eV) as calculated from finite difference pseudopotentials and as measured from atomic spectra (Ref. 25).

	Silicon	Carbon	Oxygen
E_s (FD)	−0.78	−0.99	−1.74
E_s (DI)	−0.80	−1.00	−1.74
E_p (FD)	−0.29	−0.38	−0.68
E_p (DI)	−0.31	−0.40	−0.68
$^3P\rightarrow{}^1D$ (FD)	0.77	1.31	1.87
$^3P\rightarrow{}^1D$ (Expt.)	0.78	1.26	1.84

The chief source of error from the higher-order finite-difference method arises from the finite size of R_{max}. Even if the valence charge is strongly localized, the exchange-correlation potential does not decay very rapidly. For example, consider an exchange potential which scales as $\sim\rho(r)^{1/3}$. Even if the charge falls off by three orders of magnitude at R_{max} the exchange potential decays by only one order of magnitude. By requiring the charge to vanish outside R_{max}, we also require the exchange-correlation potential to vanish beyond this radius. This error manifests itself in a small error in the resulting self-consistent potential and in the total energy of the atom. For example, in the case of atomic oxygen the "finite-difference" self-consistent potential differs by an rms error of ~0.01 Ry from the potential found by "direct integration." The total energy of the oxygen atom as calculated within the finite-difference pseudopotential is likewise different from the direct integration. In the worse case, we have found an error of ~0.1 Ry in the total energy. However, this error will exist for the molecular, or larger cluster, case. We expect relative energy

differences to be much smaller than this error. We also note that similar problems can occur for supercell approaches, i.e., the exchange correlation may not be correctly replicated unless the cell size is quite large.

III. APPLICATION TO DIATOMIC MOLECULES

The diatomic molecules were computed following the same prescription as for the atomic species. By determining the electronic energy change as function of bond length, we can find the cohesive energy, the equilibrium bond length and the vibrational modes.

In generating a self-consistent potential, we find similar issues as for basis oriented method. For example, a self-consistent screening potential for the silicon and carbon diatomic cannot be stabilized by the usual criterion for charge neutrality, i.e., by integral occupation of the lowest-energy levels. For both silicon and carbon, two molecular configurations: (a) $(1\sigma_g)^2(1\sigma_u)^2(2\sigma_g)^2(1\pi_u)^2$ and (b) $(1\sigma_g)^2(1\sigma_u)^2(1\pi_u)^4$ may "oscillate" during the iteration process for obtaining a self-consistent potential. Configuration (a) can correspond to a triplet ($^3\Sigma_g^-$) or a singlet state ($^1\Sigma_g^+$).[26] Configuration (b) corresponds to a singlet state. Two common procedures are used in such situations. One procedure is to fractionally occupy the $(2\sigma_g)$ and $(1\pi_u)$ orbitals until a stable potential is obtained. Another procedure is to fix integer occupation of the triplet or singlet configuration, and iterate either configuration to self-consistency. In the context of a spin-polarized local-density procedure, the latter procedure allows us to calculate the energy difference in the triplet and singlet states, ΔE_{sp}, via perturbation theory:

$$\Delta E_{sp} = \int \rho(x,y,z)[\epsilon_{xy}(\rho(x,y,z),\xi(x,y,z)) - \epsilon_{xc}(\rho(x,y,z),\xi(x,y,z))]dx\,dy\,dz\ , \tag{7}$$

where $\epsilon_{xc}(x,y,z)$ is the exchange-correlation density, $\rho(x,y,z)$ is the electronic charge density, and $\xi(x,y,z)$ is the spin density. We have used this latter procedure as it is easy to implement with little loss in accuracy. For the silicon dimer, we were able to reproduce previous spin-density calculations which used a plane-wave basis. We find the triplet to be the ground state. Carbon is more complex. The observed ground state is the $^1\Sigma_g^+$ state, but this state differs by only 0.08 eV from the $^3\Pi_u$ state. We find a singlet state which is consistent with previous calculations.[27] However, some recent spin-polarized calculations have yielded a triplet ground state.[28]

In Fig. 4, we illustrate the binding energy as a function of bond length for the molecules of interest. The cohesive energy from local-density calculations is not very reliable without including gradient corrections.[29] Our motivation here is not to improve on this formalism, but to test the accuracy of the finite-difference method. We have determined the cohesive energy by subtracting the energy of the constituent atoms from the molecular energy without gradient corrections. We summarize our calculated binding energy in Table IV. Typically, we find an overbinding by $\sim 1-2$ eV compared to experiment. This overbinding is reassuring in that incomplete or poorly converged bases often yield cohesive energies which are underbound compared to experiment. Only our CO molecule is slightly underbound. It may be that our grid spacing of $h = 0.4$ a.u. is slightly too large for a highly converged solution. However, our binding energy exceeds that of previous work.[31]

Bond lengths are accurately reproduced by our calculations as are the vibrational modes (see Table IV). The largest bond length discrepancy is for the carbon diatomic. This error is 0.03 Å smaller than the experimental bond length. If we were to allow fractional occupation, we would admix "triplet" character into the carbon diatomic ground state. Since the triplet state has a longer

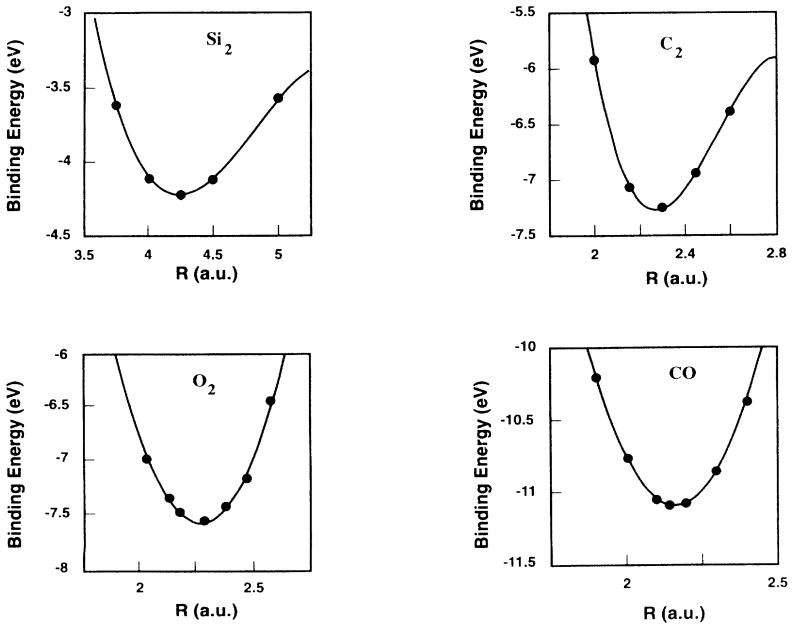

FIG. 4. Binding energy of selected diatomic molecules as function of the bond length R in a.u. (1 a.u.=0.529 Å). The calculated points (solid circles) are fit to a cubic polynomial.

TABLE IV. Properties of diatomic molecules. The experimental data are from Ref. 20. The theoretical results are from a finite-difference pseudopotential (FDP) calculation, and from other methods using similar forms for the local density approximation.

	Si_2	C_2	O_2	CO
Cohesive energy (eV)				
Experiment	3.0	6.32	5.21	11.24
FDP	4.2	7.3	7.5	11.1
Other theory	4.18[a]	7.24[b]	7.53[b]	9.6[c]
Bond length (Å)				
Experiment	2.24	1.24	1.21	1.13
FDP	2.25	1.21	1.21	1.13
Other theory	2.25[a]	1.25[b]	1.21[b]	1.17[c]
Vibrational mode (cm^{-1})				
Experiment	511	1855	1580	2170
FDP	520	1909	1630	2000
Other theory	486[a]	1903[b]	1606[b]	2100[c]

[a]From Ref. 26.
[b]From Ref. 30.
[c]From Ref. 31.

bond length than the singlet state, triplet admixture might increase the bond length. The vibrational modes were determined by fitting a cubic polynomial to the energy versus bond-length curve. The vibrational modes are accurate to within a few percent on the basis of this fitting.

Let us concentrate on a comparison between a plane-wave basis and our finite-difference "basis" for the oxygen molecule. In Fig. 5 we compare the self-consistent field, $V_{\rm loc}+V_H+V_{\rm xc}$, obtained from a supercell plane-wave calculation to one obtained using the higher-order finite-difference method. For the plane-wave calculation, a supercell of two sizes was considered. We considered supercell cubes of 12 and 24 a.u. on edge. For the finite-difference calculation a $R_{\rm max}$ of 5.6 a.u. was used, resulting in an effective cell size of 12 a.u. on edge. The only significant difference between the two potentials occurs at the atom sites, and can be attributed to the Hartree potential (see Fig. 2). The eigenvalues for an oxygen molecule as determined from the plane-wave and from the finite-difference calculations are given in Table V. Surprisingly, the orbital energies for the plane-wave calculation do not appear to be converged using a 12 a.u. cell. By increasing the cell size to 24 a.u., the orbital energies as determined by the plane-wave calculation approach the finite-difference results. The orbital energies have not been corrected for spin polarization, and correspond to the local-density eigenvalues. The energy cutoff for the plane-wave calculation was taken to be 48 Ry. For the 12-a.u. cell, $\approx$9800 plane waves were included in the calculation whereas for the 24-a.u. cell, over 77 000 plane waves were needed. This result suggests that very large supercells must be utilized to achieve converged orbital energies. It also suggests that finite-difference calculations may be more efficient for such calculations.

For the case of the oxygen molecule, we have explicitly calculated the cohesive energy, bond length, and vibrational modes via plane waves and a supercell

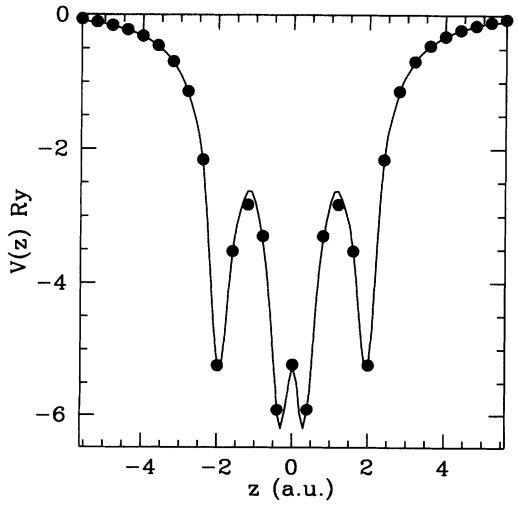

FIG. 5. The O_2 self-consistent local potential obtained form a large (24-a.u. box) supercell plane-wave calculation, solid line, and a small cell higher-order finite-difference calculation, filled dots. The oxygen atoms are at ± 1.14 a.u.

TABLE V. Orbital energies for the oxygen dimer. The orbital energies (in eV) have been calculated via higher-order finite-difference pseudopotentials, and plane-wave supercell calculations using two different supercells.

Orbital	Finite difference	Plane wave (12 a.u. supercell)	Plane wave (24 a.u. supercell)
σ_s	−32.56	−32.09	−32.60
σ_s^*	−19.62	−19.11	−19.57
σ_p	−13.63	−12.93	−13.37
π_p	−13.24	−12.54	−12.98
π_p^*	−6.35	−5.53	−5.98

configuration. For the 12-a.u. supercell, the bond length agrees within 0.01 Å. The vibrational mode also agrees to within 20 cm^{-1}. The cohesive energies do show some differences. The plane-wave value is 6.8 eV/atom as contrasted to the finite-difference value of 7.5 eV/atom. However, when the cell size is increased to a value of 24 a.u., the cohesive energy of the plane-wave result is increased to 7.2 eV/atom. This is consistent with the eigenvalue trends, i.e., the 12-a.u. supercell is not sufficient to replicate an accurate description of the oxygen molecule.

As in the case of plane-wave solutions, we can calculate the densities of individual orbitals, $|\psi(\mathbf{r})|^2$, and the total charge density of the molecule. In Fig. 6, we illustrate the charge density of the O_2 diatomic orbitals and compare directly to the plane-wave basis. The FFT grid size used for the plane-wave orbital calculation was 128, which is more than five times as dense as the finite-difference real space grid. The agreement between the two orbital sets is remarkably good, considering the differences in the grid point densities.

In Fig. 7, we compare the total charge density of the diatomic molecules as calculated from the finite-difference method to plane-wave calculations using the same pseudopotential in a supercell geometry. (The total energies, bond lengths, and vibrational frequencies agree to within computational accuracy.) The charge densities

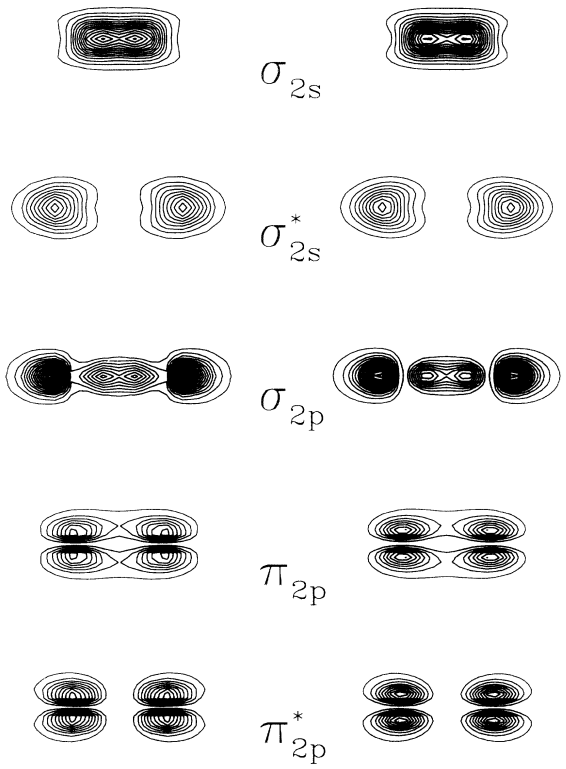

FIG. 6. Molecular orbitals for the oxygen molecule. The contour spacings are in units of 0.001 a.u. The orbitals have been calculated with a higher-order finite-difference method over a fixed grid, left figures, and with a plane-wave basis, right figures.

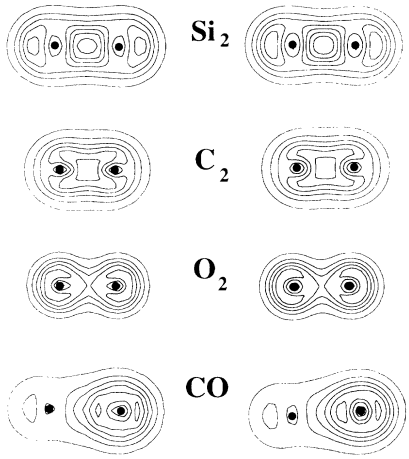

FIG. 7. Pseudo-charge densities, $|\psi(\mathbf{r})|^2$, for Si_2, C_2, O_2, and CO molecules. The left-hand side corresponds to finite-difference pseudopotential calculations; the right-hand side corresponds to pseudopotential-plane-wave calculations. The densities are in atomic units. The contour spacings are 0.0125 for Si_2, 0.05 for C_2, and 0.15 for O_2 and CO.

are nearly identical; the chief difference is a finer grid used for the plane-wave basis.

The charge density of the carbon dimer is unusual compared to other forms of carbon. In crystalline forms of carbon such as diamond and graphite the bond charge has a double "hump," i.e., a saddle point occurs in the charge density at the bond site. Large carbon clusters such as the fullerene molecule also has a double hump configuration. This bond charge configuration is unlike the configuration in other neighboring covalent materials such as silicon, or germanium. In silicon or germanium, the charge density has a maximum at the bond site. The bond charge for carbon which we calculate is more like silicon or germanium. However, this is true only for the singlet state. The carbon dimer in the triplet state does have double hump structure. In the molecular case, the occupation of the $2\sigma_g$ orbital controls whether the bond configuration results in a local maximum or saddle point structure.

It is very gratifying to note that the finite-difference wave functions reproduce the dipole moment of the CO molecule. The dipole in CO is extraordinarily sensitive to the bond length and even changes sign with changing bond length.[31] At large distances the dipole corresponds to charge configuration of C^+O^-. At smaller distance the sign reverses, and at equilibrium, the dipole corresponds to charge state of C^-O^+. The dipole we calculate is $-0.10D$ compared to the experimental value of $-0.1227D$.[32] A previous local-density calculation has given a value of $-0.01D$.[31,33] In Fig. 8, we illustrate the dipole of the CO molecule versus the interatomic separation. We compare to the experimental results, and to two other theoretical calculations: a Hartree-Fock calculation, and an all-electron local-density calculation. In Fig. 9, we plot the valence charge density of the CO molecule as a function of interatomic separation, i.e., for $R = 2.30$,

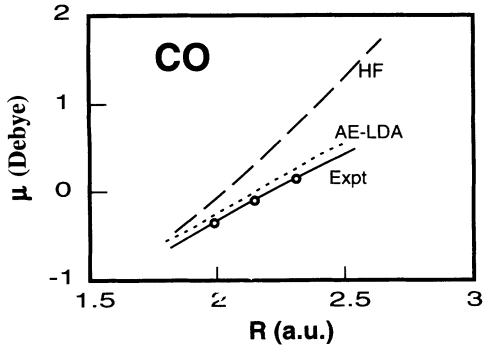

FIG. 8. Dipole of the CO molecule as a function of bond length. A positive dipole corresponds to C^+O^-. Results from two theoretical calculations and experiment are illustrated. The open circles correspond to a finite-difference calculation.

2.15, and 2.00 a.u. We can use a qualitative criterion for assessing how the covalent bond charge is altered by changing the bond length. We can define a "bond charge" by the charge within the lowest closed contour formed between the cation and anion. Under this criterion, no bond charge exists for the CO molecule at $T=2.30$ a.u. A small bond charge exists at $T=2.15$ a.u., and increases significantly at $R=2.00$ a.u. This strong rearrangement of the charge effectively transfers charge from the O anion to the CO covalent bond as the bond length is decreased.

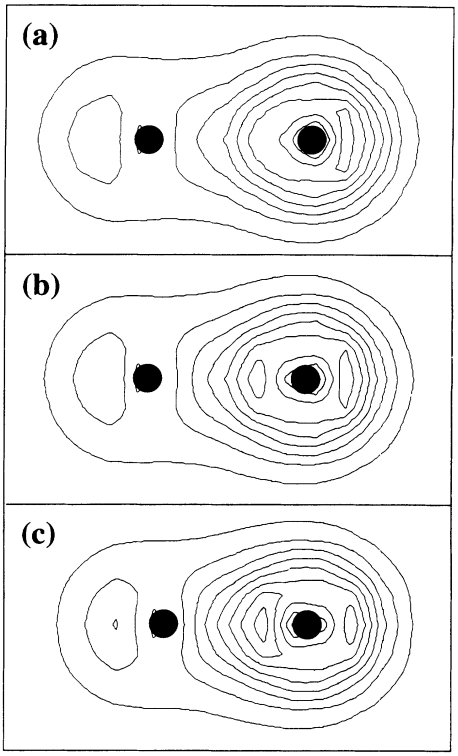

FIG. 9. Pseudo-charge-density for the CO charge density for three different bond lengths: (a) 2.30 a.u., (b) 2.15 a.u., and (c) 2.00 a.u.

IV. CONCLUSIONS

In summary, we have presented a method for performing electronic-structure calculations without the explicit use of a basis. We have combined the finite-difference approach with *ab initio* pseudopotentials. In contrast to the methods which use a plane-wave basis, our calculations are performed completely in real space. No artifacts such as supercell geometries need be introduced for localized systems. The method is applicable to charged systems. Moreover, it is much easier to implement than are plane waves, and it is more amenable to implementation on parallel computers.

ACKNOWLEDGMENTS

We would like to acknowledge support for this work by the National Science Foundation, and by the Minnesota Supercomputer Institute. We thank Dr. Bengt Fornberg for a copy of his paper on higher-order finite-difference methods prior to publication.

[1]J. R. Chelikowsky and M. L. Cohen, *Handbook on Semiconductors,* edited by P. T. Landsberg (Elsevier, Amsterdam, 1992), Vol. 1, p. 59.

[2]M. L. Cohen, M. Schlüter, J. R. Chelikowsky, and S. G. Louie, Phys. Rev. B **12**, 5575 (1975).

[3]K. M. Ho, M. L. Cohen, and M. Schlüter, Chem. Phys. Lett. **46**, 608 (1977); M. Schlüter, Z. Zunger, G. Kerker, K. M. Ho, and M. L. Cohen, Phys. Rev. Lett. **42**, 540 (1979).

[4]I. Stich, R. Car, and M. Parrinello, Phys. Rev. B **44**, 4262 (1991); Phys. Rev. Lett. **63**, 2240 (1989).

[5]J. R. Chelikowsky and N. Binggeli, Solid State Commun. **88**, 381 (1993); J. R. Chelikowsky, N. Troullier, and N. Binggeli, Phys. Rev. B **49**, 114 (1994).

[6]I. Stich, M. C. Payne, R. D. King-Smith, J.-S. Lin, and L. J. Clarke, Phys. Rev. Lett. **68**, 1351 (1992).

[7]K. D. Brommer, M. Needels, B. E. Larson, and J. D. Joannopoulos, Phys. Rev. Lett. **68**, 1355 (1992).

[8]N. Binggeli, J. L. Martins, and J. R. Chelikowsky, Phys. Rev. Lett. **68**, 2956 (1992).

[9]This approach has been used to study charged impurities see, e.g., C. G. Van de Walle, P. J. H. Denteneer, Y. Bar-Yam, and S. T. Pantelides, Phys. Rev. B **39**, 10 791 (1989); S. Froyen and A. Zunger, *ibid.* **34**, 7451 (1986).

[10]G. D. Smith, *Numerical Solutions of Partial Differential Equations: Finite Difference Methods,* 2nd ed. (Oxford, New York, 1978).

[11]J. R. Chelikowsky, N. Troullier, and Y. Saad, Phys. Rev. Lett. **72**, 1240 (1994).

[12]G. E. Kimball and G. H. Shortley, Phys. Rev. **45**, 815 (1934).

[13]The most notable of these early authors are G. E. Kimball, G.

H. Shortley, J. H. Bartlett, R. P. Bell, and D. R. Hartree. This list is by no means complete. The limited number of early works in this numerical area is due mainly to the lack of computational devices.

[14]D. E. Ellis and G. S. Painter, Phys. Rev. B **2**, 2887 (1970); G. S. Painter, D. E. Ellis, and A. R. Lubinsky, *ibid.* **4**, 3610 (1971).

[15]J. V. Lill, G. A. Parker, and J. C. Light, Chem. Phys. Lett. **89**, 483 (1982).

[16]It is not necessary to impose a uniform 3D grid upon the present problem. However, given the added complexity of a nonuniform grid and the smoothly varying nature of the pseudopotentials and wave functions, we find that it is more advantageous to use a simple uniform 3D grid. A nonorthogonal grid could also have been used, which would have only slightly increased the computational workload, but in the present case it is not needed.

[17]B. Fornberg and D. M. Sloan, in *Acta Numerica 94,* edited by A. Iserles (Cambridge University Press, Cambridge, in press).

[18]D. M. Ceperley and B. J. Alder, Phys. Rev. Lett. **45**, 566 (1980); J. P. Perdew and A. Zunger, Phys. Rev. B **23**, 5048 (1981).

[19]N. Troullier, Y. Saad, and J. R. Chelikowsky (unpublished).

[20]For a periodic system, one uses a similar approach for solving the Poisson equation. The matrix is set up with periodic boundary conditions and the total charge within the cell is zero. This is done to offset the infinite summation in setting up the periodic ionic potential, i.e., following the same reasoning and methodology as in using a plane-wave basis.

[21]C. G. Broyden, Math. Comp. **19**, 577 (1965).

[22]N. Troullier and J. L. Martins, Phys. Rev. B **43**, 1993 (1991).

[23]L. Kleinman and D. M. Bylander, Phys. Rev. Lett. **48**, 1425 (1982).

[24]N. Troullier and J. L. Martins, Phys. Rev. B **43**, 8861 (1991).

[25]C. E. Moore, *Atomic Energy Levels,* Natl. Bur. Stand. Ref. Data Ser. Natl. Bur. Stand. (U.S.) Circ. No. 467 (U.S. GPO, Washington, D.C., 1949), Vol. 1.

[26]J. E. Northrup, M. T. Yin, and M. L. Cohen, Phys. Rev. A **28**, 1945 (1983).

[27]J. R. Chelikowsky and M. Y. Chou, Phys. Rev. B **37**, 6504 (1988).

[28]F. W. Kutzler and G. S. Painter, Phys. Rev. B **45**, 3236 (1992).

[29]K. P. Huber and G. Herzberg, *Constants of Diatomic Molecules* (Van Nostrand, New York, 1979).

[30]S. H. Vosko, L. Wilk, and M. Nusair, Can. J. Phys. **58**, 1200 (1980).

[31]O. Gunnarsson, J. Harris, and R. O. Jones, J. Chem. Phys. **67**, 3970 (1977).

[32]C. Charkerian, Jr., J. Chem. Phys. **65**, 4228 (1976).

[33]A recent chemistry multiconfigurational self-consistent-field averaged coupled pair functional (MCSCF-ACPF) calculation gives $-0.12D$ for the CO dipole. Given the simplicity of the local-density approximation (LDA) calculations as compared to MCSCF-ACPF, the current LDA dipole results are in excellent agreement with experiment.